Available online at www.sciencedirect.com
SCIENCE DIRECT®
Carbohydrate Research 340 (2005) 2376–2391
Carbohydrate RESEARCH

Crystalline structure analysis of cellulose treated with sodium hydroxide and carbon dioxide by means of X-ray diffraction and FTIR spectroscopy

Sang Youn Oh,[a] Dong Il Yoo,[a,*] Younsook Shin,[b] Hwan Chul Kim,[c] Hak Yong Kim,[c] Yong Sik Chung,[c] Won Ho Park[d] and Ji Ho Youk[e]

[a]*Department of Textile Engineering, Chonnam National University, Gwangju, 500-757, Republic of Korea*
[b]*Department of Clothing & Textiles, Chonnam National University, Gwangju, 500-757, Republic of Korea*
[c]*Department of Textile Engineering, Chonbuk National University, Jeonju, 561-756, Republic of Korea*
[d]*Department of Textile Engineering, Chungnam National University, Daejeon, 305-764, Republic of Korea*
[e]*Department of Textile Engineering, Inha University, Incheon, 402-751, Republic of Korea*

Received 21 December 2004; accepted 14 August 2005
Available online 8 September 2005

Abstract—Crystalline structures of cellulose (named as Cell 1), NaOH-treated cellulose (Cell 2), and subsequent CO_2-treated cellulose (Cell 2-C) were analyzed by wide-angle X-ray diffraction and FTIR spectroscopy. Transformation from cellulose I to cellulose II was observed by X-ray diffraction for Cell 2 treated with 15–20 wt % NaOH. Subsequent treatment with CO_2 also transformed the Cell 2-C treated with 5–10 wt % NaOH. Many of the FTIR bands including 2901, 1431, 1282, 1236, 1202, 1165, 1032, and 897 cm^{-1} were shifted to higher wave number (by 2–13 cm^{-1}). However, the bands at 3352, 1373, and 983 cm^{-1} were shifted to lower wave number (by 3–95 cm^{-1}). In contrast to the bands at 1337, 1114, and 1058 cm^{-1}, the absorbances measured at 1263, 993, 897, and 668 cm^{-1} were increased. The FTIR spectra of hydrogen-bonded OH stretching vibrations at around 3352 cm^{-1} were resolved into three bands for cellulose I and four bands for cellulose II, assuming that all the vibration modes follow Gaussian distribution. The bands of 1 (3518 cm^{-1}), 2 (3349 cm^{-1}), and 3 (3195 cm^{-1}) were related to the sum of valence vibration of an H-bonded OH group and an intramolecular hydrogen bond of 2-OH···O-6, intramolecular hydrogen bond of 3-OH···O-5 and the intermolecular hydrogen bond of 6-O···HO-3′, respectively. Compared with the bands of cellulose I, a new band of 4 (3115 cm^{-1}) related to intermolecular hydrogen bond of 2-OH···O-2′ and/or intermolecular hydrogen bond of 6-OH···O-2′ in cellulose II appeared.

The crystallinity index (CI) was obtained by X-ray diffraction [CI(XD)] and FTIR spectroscopy [CI(IR)]. Including absorbance ratios such as $A_{1431,1419}/A_{897,894}$ and $A_{1263}/A_{1202,1200}$, the CI(IR) was evaluated by the absorbance ratios using all the characteristic absorbances of cellulose. The CI(XD) was calculated by the method of Jayme and Knolle. In addition, X-ray diffraction curves, with and without amorphous halo correction, were resolved into portions of cellulose I and cellulose II lattice. From the ratio of the peak area, that is, peak area of cellulose I (or cellulose II)/total peak area, CI(XD) were divided into CI(XD-CI) for cellulose I and CI(XD-CII) for cellulose II. The correlation between CI(XD-CI) (or CI(XD-CII)) and CI(IR) was evaluated, and the bands at 2901 (2802), 1373 (1376), 897 (894), 1263, 668 cm^{-1} were good for the internal standard (or denominator) of CI(IR), which increased the correlation coefficient. Both fraction of the absorbances showing peak shift were assigned as the alternate components of CI(IR). The crystallite size was decreased to constant value for Cell 2 treated at $\geqslant$15 wt % NaOH. The crystallite size of Cell 2-C (cellulose II) was smaller than that of Cell 2 (cellulose I) treated at 5–10 wt % NaOH. But the crystallite size of Cell 2-C (cellulose II) was larger than that of Cell 2 (cellulose II) treated at 15–20 wt % NaOH.
© 2005 Elsevier Ltd. All rights reserved.

Keywords: Cellulose; Sodium hydroxide; Carbon dioxide; X-ray diffraction; FTIR; Crystallinity index (CI); Resolution; Cellulose I; Cellulose II

* Corresponding author. Tel.: +82 62 530 1773; fax: +82 62 530 1779; e-mail: diyoo@chonnam.ac.kr

0008-6215/$ - see front matter © 2005 Elsevier Ltd. All rights reserved.
doi:10.1016/j.carres.2005.08.007

1. Introduction

Cellulose is a linear homopolymer of (1→4)-linked β-D-glucopyranose units (Glc) aggregated to form a highly ordered structure due to its chemical constitution and spatial conformation.[1] Three hydroxyl groups in each Glc are able to interact with one another forming intra- and intermolecular hydrogen bonds. The use of cellulose in some applications is limited because it is soluble in a few solvents and does not melt without thermal degradation. Hydrogen bonds in cellulose substrates are modified by some physical and/or chemical transformations for various applications. Typically, treatment with aqueous NaOH solution of a specific concentration (~10 wt %) causes the transformation of cellulose I into cellulose II within the crystalline domains.[2–4] This procedure is used for mercerization and viscose rayon manufacture in the textile and fiber industries.[5,6] However, the concentration of NaOH for the complete transformation depends on the type of cellulose being treated.

Common methods for the characterization of crystalline cellulose structure are based on X-ray[4,7–19] or electron diffraction[19–21] FT Raman,[3,21–23] density determinations, infrared (IR) absorption,[10,14,15,17,19,21–33] nuclear magnetic resonance (NMR),[21,34] and calorimetry. Among them, wide-angle X-ray diffraction gives the most direct results; however, its interpretation is still under discussion. Adopting two-phase structure theory and the amorphous halo correction, the crystallinity index (CI) is obtained from X-ray diffraction curves by using the method of Jayme and Knolle.[35] Though X-ray diffraction gives quantitative information, complementary approaches are introduced for the analysis of hydrogen-bond and spatial conformations between cellulose molecules. FTIR absorption, as well as NMR spectroscopy, gives some useful information related to the change of hydrogen bonding during crystal transformation. Until now there has been no remarkable research correlating the CI obtained between X-ray diffraction [CI(XD)] and other methods.

We treated NaOH-treated cellulose with CO_2 and successfully dissolved it in aqueous NaOH solution.[36] Physical and chemical changes of the cellulose (named as Cell 1), NaOH-treated cellulose (Cell 2), and subsequent CO_2-treated cellulose (Cell 2-C) were elucidated by FTIR analysis.[37] Hydrogen-bond intensity (HBI) and CI measured by $A_{4000-2995}/A_{1337}$ or $(A_{4000-2995}/A_{993})$ and A_{1430}/A_{900}, respectively, were evaluated for the study of physical changes. In the study of chemical changes, the introduction of the hydrogen-bonded asymmetric carbonyl stretching and O–C–O stretching of the carbonate ion at 1593 and 1470 cm^{-1}, respectively, in the CO_2-treated celluloses was elucidated by FTIR spectroscopy in an instrument equipped with an on-line evacuation apparatus. In this study, crystalline structures of these cellulose samples are characterized by X-ray diffraction and FTIR. The CI was obtained by X-ray diffraction [CI(XD)] and FTIR [CI(IR)]. The CI(IR) was evaluated by the absorbance ratios using all the characteristic absorbances of the celluloses. The CI(XD) was calculated by the method of Jayme and Knolle.[35] The cellulose I and cellulose II components were resolved using X-ray diffraction patterns, and then correlations between CI(XD-CI) for the cellulose I component or CI(XD-CII) for the cellulose II component and CI(IR) were researched. Finally, the size of the crystallites was determined from 101, 10$\bar{1}$, 002, and 021 lattice planes of the celluloses.

2. Experimental

2.1. Materials

Pulp sheet (Cellunier-F®, Rayonier Fernandina Mill, USA, DP 850, 92% α-cellulose) commonly used in viscose process was shredded to the form of powder (*Φ* 1 mm). Oven-dried (at 60 °C) cellulose powder was used. Commercially available compressed CO_2 gas was used for the reaction with cellulose. Analytical-grade reagents such as NaOH and *N*,*N*-dimethylacetamide (DMAc) were used as received.

2.2. Reaction of cellulose with NaOH and CO_2

Ca. 15 g of cellulose powder (Cell 1) was treated with 500 mL of NaOH solution at 25 or 60 °C for 1 h and then filtered to get NaOH-treated cellulose (NC). The concentrations of the NaOH solutions chosen were 5, 10, 15, and 20 wt %. NC was washed with excess water up to pH 7 for filtrates to obtain the Cell 2 sample. The Cell 1 (or filtered NC) in 300 mL of DMAc was treated with 40–50 bar of CO_2 in a high pressure reactor at −5 to 0 °C stirring for 2 h and then washed with an excess water up to pH 7. Cell 1-C from Cell 1 (or Cell 2-C from NC) obtained by the above procedure was oven dried at 60 °C.

2.3. X-ray diffraction analysis

Crystalline structures of the cellulose samples (listed in Table 1) were analyzed by wide-angle X-ray diffraction on a Rigaku-D/MAX instrument (Uitima III, Japan) with 5°/min scan speed. These cellulose samples prepared by powder were laid on the glass sample holder (35 × 50 × 5 mm) and analyzed under plateau conditions. Ni-filtered Cu Kα radiation ($\lambda = 1.54$ Å) generated at a voltage of 40 kV and current of 40 mA was utilized, and a scan speed of 2°/min from 5° to 50° was used.

Crystalline allomorphs of cellulose were determined by the resolution of wide-angle X-ray diffraction curves. The determination of CI(XD) is taken from the method

Table 1. Treatment processes for the samples used in this study[a]

Sample code	NaOH		CO_2/DMAc	Washing/drying
	25 °C	60 °C		
Cell 1	×	×	×	○
Cell 2/25	○	×	×	○
Cell 2/60	×	○	×	○
Cell 1-C	×	×	○	○
Cell 2/25-C	○	×	○	○
Cell 2/60-C	×	○	○	○

[a] ○ = treated; × = untreated.

of Jayme and Knolle.[35] Amorphous halos were drawn by the Microcal™ ORIGIN™ program for the determination of h_{am}. CI(XD) was calculated by (Eq. 1)

$$\mathrm{CI(XD)} = 1 - h_{am}/h_{cr} = 1 - h_{am}/(h_{tot} - h_{am}), \quad (1)$$

where the crystalline scatter of the 002 reflection at 2θ of 22.5° for cellulose I or 101 reflection at 2θ of 19.8° for cellulose II (crystalline height, h_{cr}) with the height of the 'amorphous reflection' at 2θ of 18° for cellulose I or 16° for cellulose II (amorphous height, h_{am}), respectively.[35] With and without amorphous halo correction, deconvolution of the X-ray diffraction curves was performed by using Microcal™ ORIGIN™ (Microcal Software, Inc.). Taking the Lorentzian distribution function as the shape of the resolved bands, cellulose I and cellulose II components were resolved into four and three reflections, respectively (Fig. 10). From the sum of peak area of the same crystal system (ΣA_{CI} for cellulose I, ΣA_{CII} for cellulose II), CI(XD) are divided into CI(XD-CI) for cellulose I and CI(XD-CII) for cellulose II. The components obtained without amorphous halo correction are denoted CI(XD-CI′) and CI(XD-CII′), respectively (Eq. 2).

$$\begin{aligned}\mathrm{CI(XD\text{-}CI)} &= \frac{\Sigma A_{CI}}{\Sigma(A_{CI} + A_{CII})} \times \mathrm{CI(XD)} \\ \mathrm{CI(XD\text{-}CII)} &= \frac{\Sigma A_{CII}}{\Sigma(A_{CI} + A_{CII})} \times \mathrm{CI(XD)}\end{aligned} \quad (2)$$

The crystallite size was calculated from the Scherrer equation with the method based on the width of the diffraction patterns (Eq. 3). The crystallites sizes were determined from the 101, $10\bar{1}$, 002, and 021 lattice planes of cellulose samples.[10,38,39]

$$D_{(hkl)} = \frac{k\lambda}{B_{(hkl)} \cos\theta} \quad (3)$$

where $D(hkl)$ is the size of crystallite (nm), k is the Scherrer constant (0.94), λ is X-ray wavelength, $B(hkl)$ is the full-width at half-maximum of the reflection hkl measured in 2θ is the corresponding Bragg angle.[10,38,39]

2.4. FTIR analysis

Pellets of ca. 2 mg of cellulosic samples were prepared by mixing with 200 mg of spectroscopic grade KBr. FTIR spectra were recorded using a Nicolet 520P spectrometer with detector at 4 cm^{-1} resolution and 64 scans per sample.

The spectra of same absorbance intervals were shifted parallel to the wave number axis. The FTIR spectra (3900–2990 cm^{-1}) were resolved by using a Gaussian distribution function into three or four bands having similar values of wave number at maximum absorbance and band width at half maximum. Absorbance of the band obtained from a local baseline between adjacent valleys was automatically calculated at the maximum absorbance found by sensitivity of 100 using OMNIC 4.0 software.[36] CI obtained by FTIR, CI(IR), was evaluated from the ratios of the absorption bands such as A_{1430}/A_{894}, $A_{1278,1282}/A_{1263}$, and A_{1372}/A_{894}. As the internal standards, the bands at 2901 (2892), 1373 (1376), 897 (894), 1263, 668 cm^{-1} were selected.

3. Results and discussion

3.1. X-ray diffraction and FTIR analysis of the cellulose treated with NaOH and CO_2

We reported previously that all the factors affecting the solubility of cellulose samples by carbon dioxide treatment were examined to get better dissolution.[36] As a result of NaOH treatment, hydrogen-bond intensity of the cellulose is increased. For the cellulose samples treated with CO_2, new bands at 1593 and 1470 cm^{-1} are assigned as hydrogen-bonded carbonyl stretching and the O–C–O stretching of the carbonate ion, respectively.[37] These bands confirm the carbonation reaction for the cellulose samples treated with CO_2.

X-ray diffraction curves and FTIR spectra in 1480–640 cm^{-1} region of Cell 1 and Cell 1-C are shown in Figure 1. Both diffraction curves are of typical cellulose I structure. Though carbonation is introduced, CO_2 treatment does not produce any significant changes in the FTIR spectrum of cellulose in 1480–640 cm^{-1} region.

X-ray diffraction curves of the cellulose samples treated with NaOH and/or CO_2 are shown in Figure 2. At the treatment of $\geqslant$15 wt % NaOH, the crystal system of the Cell 2/25 (or Cell 2/60) is changed into cellulose II. When CO_2 treatment follows, it is transformed to cellulose II for the Cell 2/25-C and Cell 2/60-C treated with $\geqslant$10 wt % NaOH at 25 °C and $\geqslant$5 wt % NaOH at 60 °C, respectively (Fig. 2b and d). The crystalline structure of cellulose treated with $\leqslant$10 wt % NaOH is transformed to cellulose II by the CO_2 treatment that follows.

FTIR spectra in 1480–640 cm^{-1} region are shown for the Cell 2 and Cell 2-C treated by NaOH at 25 °C (Fig. 3) and 60 °C (Fig. 4). By the transformation, many characteristic bands are shifted at the peak maximum or the absorbance is changed as shown in Table 2. The bands at 1431, 1373, 1282, 1236, 1202, 1165, 1032, and

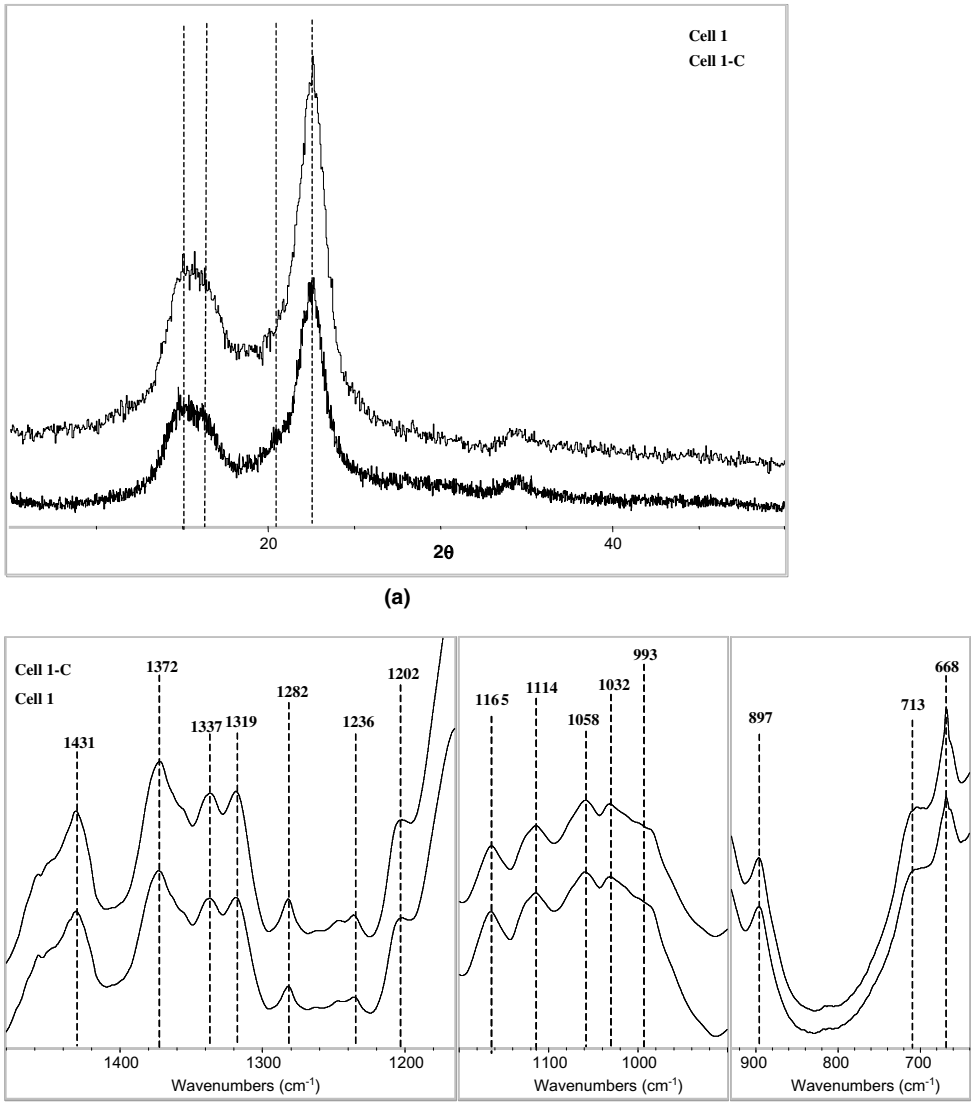

Figure 1. (a) Wide-angle X-ray diffraction curves and (b) FTIR spectra (1480–640 cm^{-1}) of Cell 1 and Cell 1-C.

897 cm^{-1} are shifted to 1419, 1376, 1278, 1228, 1200, 1162, 1019, and 894 cm^{-1}, respectively. Including the shift of O–H and C–H stretching vibrations (3352→3447, 2901→2892 cm^{-1}), all the bands are influenced by the transformation related to the change of intra- and intermolecular bonds. The change of O–H stretching and bending modes by carbonation has already been discussed.[37]

With a few exceptions (the bands at 3352, 2901, 1202, and 897 cm^{-1}), many of the bands at 1431, 1373, 1337, 1319, 1282, 1236, 1165, 1114, 1058, 1032, 713 cm^{-1} are decreased. Absorbances of the bands at 1337, 1114, and 1058 cm^{-1} are decreased, but some other bands at 1263, 993, and 668 are increased by the transformation. Typical changes related to the cellulose II transformation are shown in Figure 5. Some of the bands in Figures 3 and 4 show the change of absorbance like (a) 1337 cm^{-1} (decrease) or (b) 668 cm^{-1} (increase). In addition to absorbance change, wave number shifts are also shown for the other bands at (a) 1373→1376 cm^{-1} (higher wave number, absorbance decrease) and (b) 897→894 cm^{-1} (lower wave number, absorbance increase).

3.2. Characterization of the characteristic FTIR bands changed by transformation

Various reactions such as the inclusion of alkali and water in the cellulose and the splitting and formation of new inter- and intramolecular hydrogen bonds have been reported by Fengel.[33,41–43] regarding the absorbance variations and wave number shifts in the FTIR

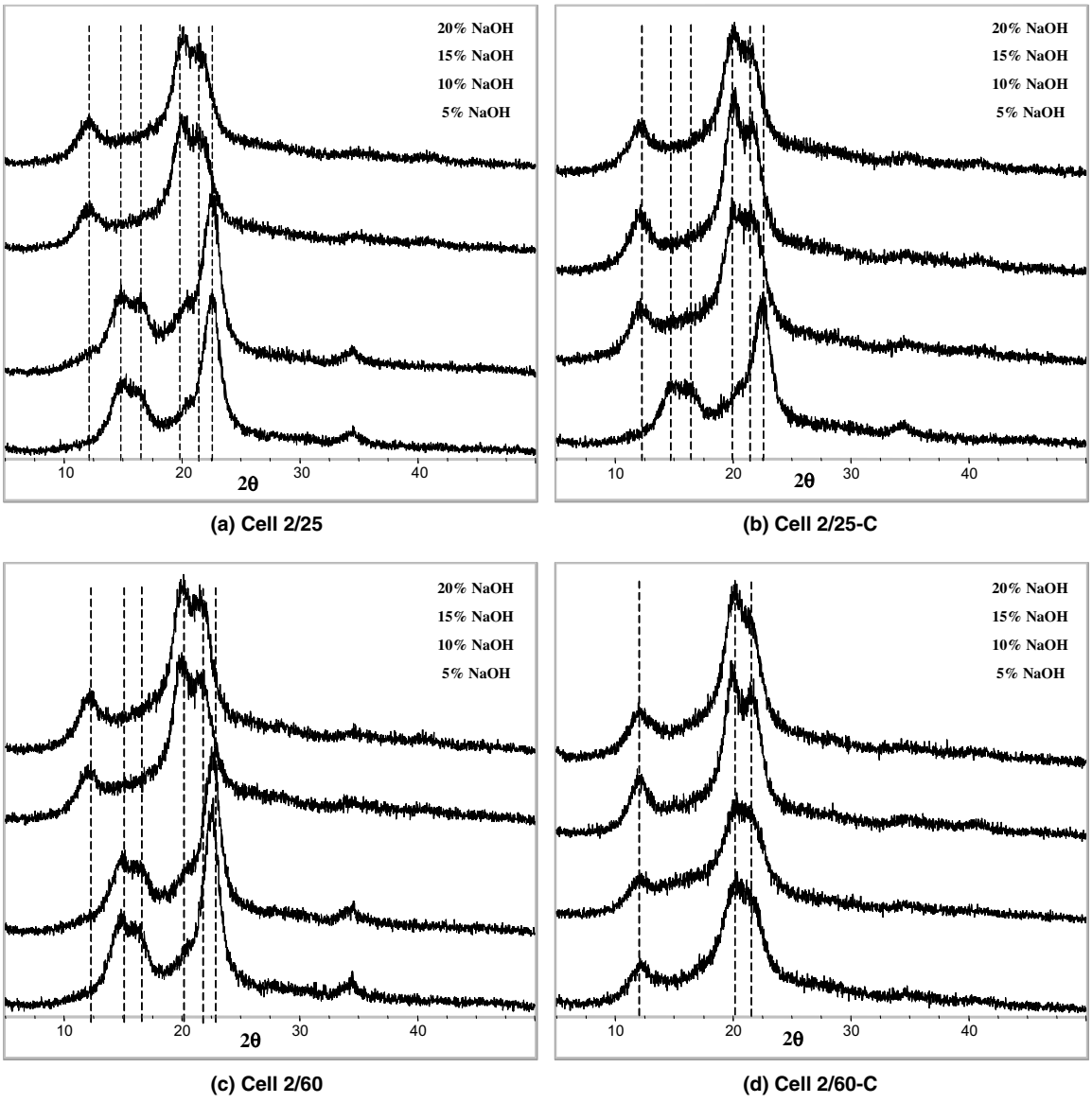

Figure 2. (a) Wide-angle X-ray diffraction curves of Cell 2/25, (b) Cell 2/25-C, (c) Cell 2/60, and (d) Cell 2/60-C.

spectra. In this study, the intramolecular hydrogen bonds for 2-OH···O-6 and 3-OH···O-5, and the intermolecular hydrogen bonds for 6-OH···O-3′ in cellulose I appear at 3455–3410, 3375–3340, and 3310–3230 cm^{-1}, respectively, along with the valence vibration of H-bonded OH groups at 3570–3450 cm^{-1}.[24,27] For Cell 2, the maximum absorbance of hydrogen-bonded O–H stretching is shifted to higher wave number (3352→3447 cm^{-1}) when treated at higher NaOH concentration (Fig. 6).[33,40] For both treatment temperatures, the maximum absorbance of O–H stretching is shifted to 3447 cm^{-1} due to the intramolecular hydrogen bond of 2-OH···O-6 by transformation. The band at 3310–3230 cm^{-1} (intermolecular hydrogen bond of 6-OH···O-3′) overlaps with the bands due to the intramolecular hydrogen bond.

Figure 7 shows the FTIR spectra of hydrogen-bonded O–H stretching vibrations with the correction of baseline. Assuming that all the vibration modes follow a Gaussian distribution, mixed modes of hydrogen-bonded O–H stretching are resolved into three bands for cellulose I and four bands for cellulose II. The resolution produces similar wave number and band width at half maximum for both crystal systems. In Figure 7a, bands of 1 (3518 cm^{-1}), 2 (3349 cm^{-1}), and 3 (3195 cm^{-1}) are related to the sum of the valence vibration of H-bonded OH groups[27,41] and the intramolecular hydrogen bond of 2-OH···O-6, the intramolecular hydrogen bond of 3-OH···O-5, and the intermolecular hydrogen bond of 6-OH···O-3′, respectively.[33,42,43] Compared with the bands of cellulose I, a new band of 4 (3115 cm^{-1}) related to intermolecular hydrogen

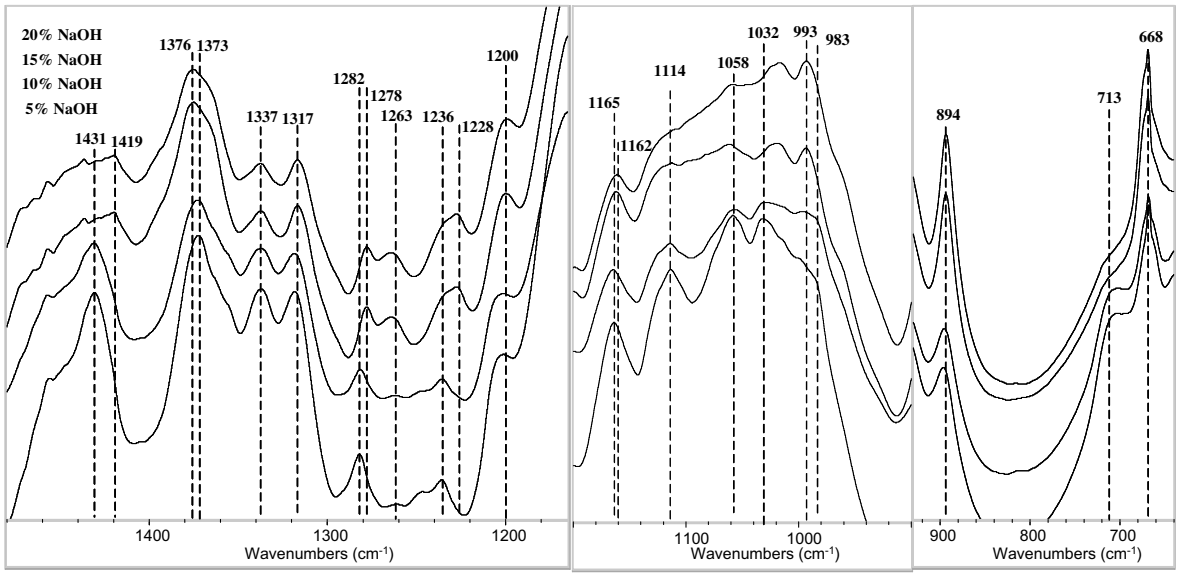

(a) Cell 2/25

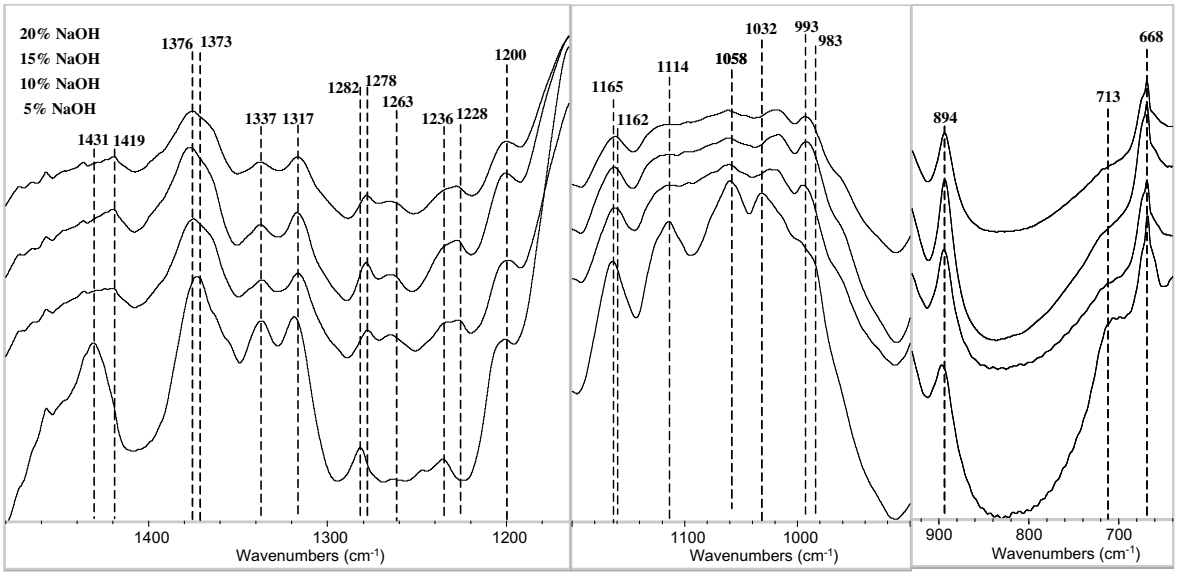

(b) Cell 2/25-C

Figure 3. (a) FTIR spectra (1480–640 cm^{-1}) of Cell 2/25 and (b) Cell 2/25-C.

bond of 2-OH···O-2′ and/or intermolecular hydrogen bond of 6-OH···O-2′ in cellulose II appears as shown in Figure 7b. The absorbance of band at 3-OH···O-5 is decreased by transformation, while the absorbances of the others are rarely changed. In addition, absorbances of the 6-OH···O-3′ band for Cell 1-C or Cell 2-C are also decreased when compared with that for Cell 1 or Cell 2, respectively. Some researchers maintain that the new band of cellulose II may be related to the intermolecular hydrogen bond of 2-OH···O-2′, which appears changed in the rotational conformation of the CH_2OH groups.[7,10,11] Newly formed 2-OH···O-2′ and 6-OH···O-2′[7] hydrogen bonds are shown along the 110 plane for the proposed hydrogen-bonding network in cellulose. As shown in Figure 8, Kolpak and Blackwell proposed that an antiparallel chain structure is the acceptable model of cellulose II model in contrast to the parallel chain system of cellulose I.[7] In the cellulose II model proposed by Kolpak and Blackwell, the *tg* (trans–gauche) conformation is retained by alternate (down) sheets, while the other (up) sheets have the *gt* (gauche–trans) conformation. The intramolecular hydrogen bond of 2-OH···O-6 shown in Figure 7 is probable in the 'down' sheets of cellulose II and cellulose I. But the C-6 resonance by ^{13}C NMR spectroscopy occurs as a singlet near 64 ppm and not as the expected

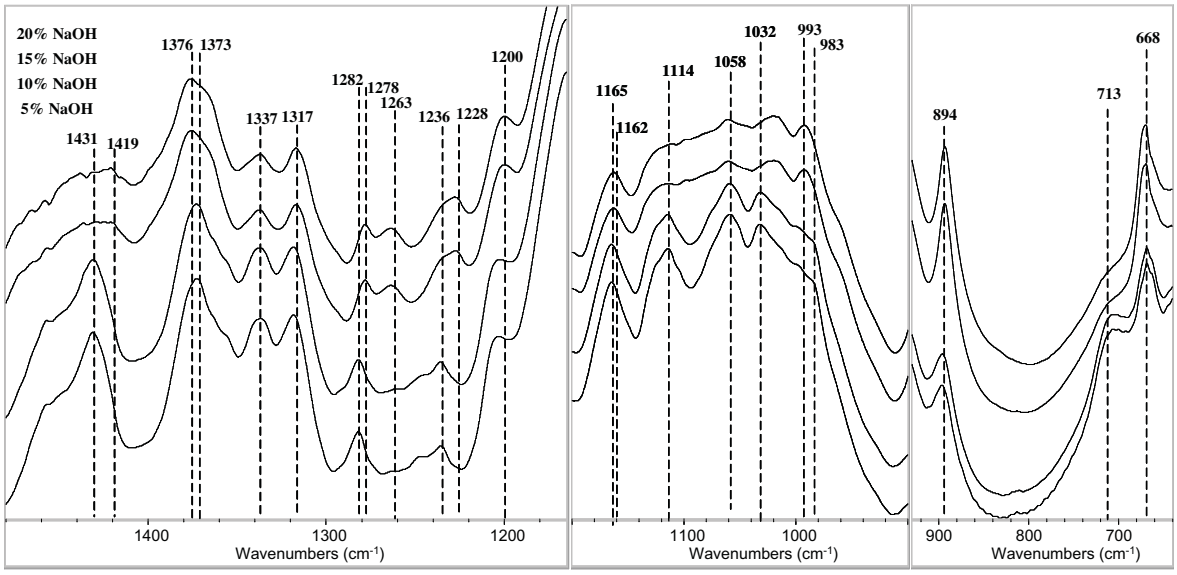

(a) Cell 2/60

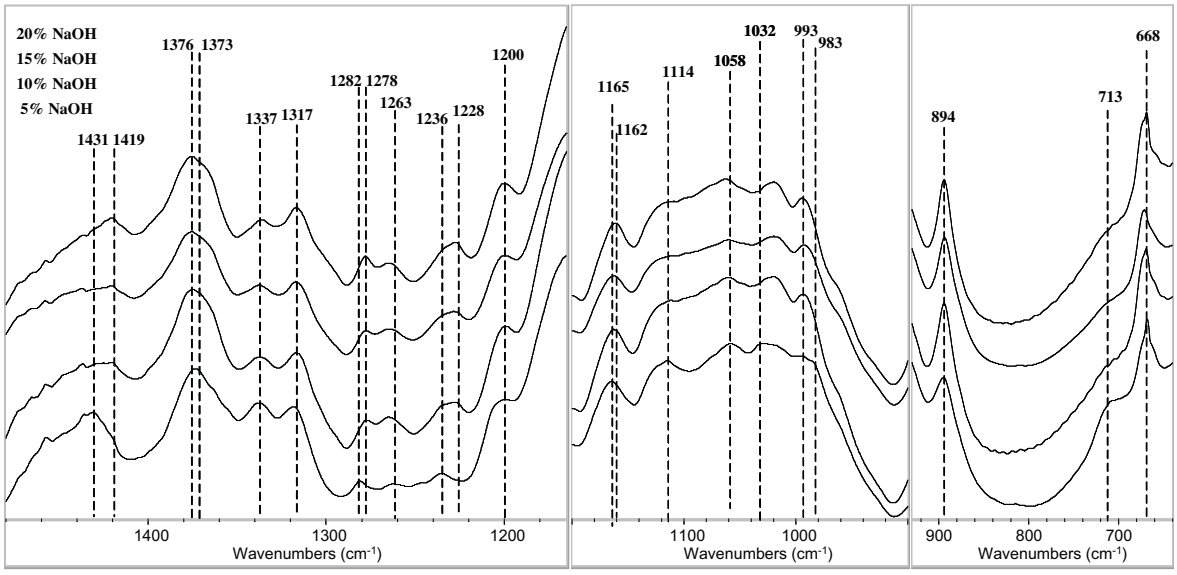

(b) Cell 2/60-C

Figure 4. (a) FTIR spectra (1480–640 cm^{-1}) of Cell 2/60 and (b) Cell 2/60-C.

doublet with a resonance near 64 and 66 ppm if both the *gt* and *tg* conformations are coexistent in the crystalline structure of cellulose II.[4,44] This indicates that there is no intramolecular hydrogen bond of 2-OH···O-6 in cellulose II.[44–46] However, the intramolecular hydrogen bonds of 2-OH···O-6 are shown in the FTIR spectra of all the cellulose samples listed in Table 2. This is explained in that the transformation (cellulose I→cellulose II) is not complete by NaOH treatment or NaOH–CO_2 treatment of the cellulose samples used in this study. Krässig reviewed previous researches and assumed carefully that heterogeneously mercerized cellulose always contains residual cellulose I structure.[35] It is generally known that high temperature and low concentration of NaOH treatment retards the transformation,[47] and treatment at elevated temperature offers more even penetration and consequently better uniformity of mercerization because of lower swelling level.[47] On the contrary, cellulose precipitated from solution such as regular viscose rayon or cellulose by saponification of cellulose acetate shows pure cellulose II structure.[35] For the analysis of incomplete transformation, we resolved cellulose I and cellulose II components by X-ray diffraction patterns and correlated them with FTIR data.

The band at 1431 cm^{-1} and 1319 cm^{-1} assigned as symmetric CH_2 bending[22,24–26,28] and CH_2 wagging[28,48] are shifted to lower wave numbers such as 1419 and

Table 2. Band characteristics of FTIR spectra related to transformation (cellulose I→cellulose II) by NaOH treatment[a]

Characteristics	ν (cm^{-1}) related to the crystal system		$\Delta\nu$ (cm^{-1})/absorbance change	Assignment	References
	Cellulose I	Cellulose II			
Peak shift	3352	3447	+95/–	γOH (hydrogen bonded)	24,25
	2901	2892	–9/–	γCH	24,27
	1431	1419	–12/∇	δCH_2 (sym) at C–6	22,24–26,28
	1373	1376	+3/∇	δC–H	24,28
	1319	1317	–2/∇	δCH_2 (wagging) at C–6	28,48
	1282	1278	–4/∇	δC–H	28
	1236	1228	–8/∇	δCOH in plane at C–6	28[b]
	1202	1200	–2/–	δCOH in plane at C–6	49[b]
	1165	1162	–3/∇	γCOC at β-glucosidic linkage	25,29,48
	1032	1019	–13/∇	γCO at C–6	31,48
	983	993	+10/Δ	γCO at C–6	49[b]
	897	894	–3/Δ	γCOC at β-glycosidic linkage. γCOC, γCCO, and γCCH at C–5 and C–6	23,25,26,28,48
Absorbance change	1337	1337	∇	δCOH in plane at C–2 or C–3	22,28
	1263	1263	Δ	δCOH in plane at C–2 or C–3	49[b]
	1114	1114	∇	γring in plane	25,49
	1058	1058	∇	γCO at C-3. γC–C	31,49
	713	713	∇	δCOH out of plane (cellulose Iβ)	10,27
	668	668	Δ	δCOH out of plane	24

[a] Key to symbols: γ: stretching, δ: bending, Δ: increase, ∇: decrease.
[b] This study.

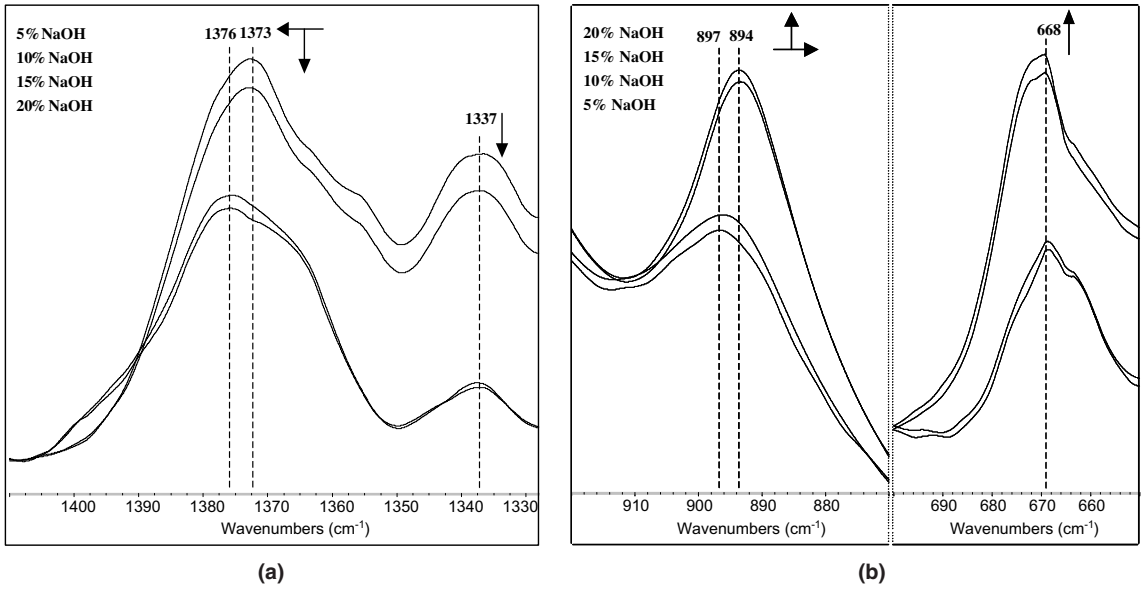

Figure 5. FTIR spectra of Cell 2/25 (a) (1450–1320 cm^{-1}) and (b) (920–870 and 700–650 cm^{-1}).

1317 cm^{-1}, respectively, when cellulose samples are treated with higher NaOH concentration as shown in Figures 3 and 4. Shift to 1419 cm^{-1} indicates development of new inter- and intramolecular hydrogen bonds and a change of the conformation of CH_2OH at C-6 from the *tg* to the *gt* form.[7,26] By this transformation, changes in absorbance and dichroic ratio are observed for the bands at 1426 and 1334 cm^{-1}.[28] The band at 2901 cm^{-1}, assigned as C–H stretching,[24,27] is shifted to 2892 cm^{-1} at higher NaOH concentrations. The band at 1431 cm^{-1} and 1319 cm^{-1} assigned as symmetric CH_2 bending[22,24–26,28] and CH_2 wagging[28,48] are shifted to lower wave numbers such as 1419 and 1317 cm^{-1}, respectively. The bands at 1337 cm^{-1},[22,28] 1263, or 713[11,26] cm^{-1}, all assigned as C–O–H bending, are also decreased.

The band at 897 cm^{-1} assigned as C–O–C stretching at the β-(1→4)-glycosidic linkage[23,25,26,28] moves toward 894 cm^{-1} by transformation as shown in Figures 3 and 4. The bands at 898 cm^{-1} and 894 cm^{-1} are shown in

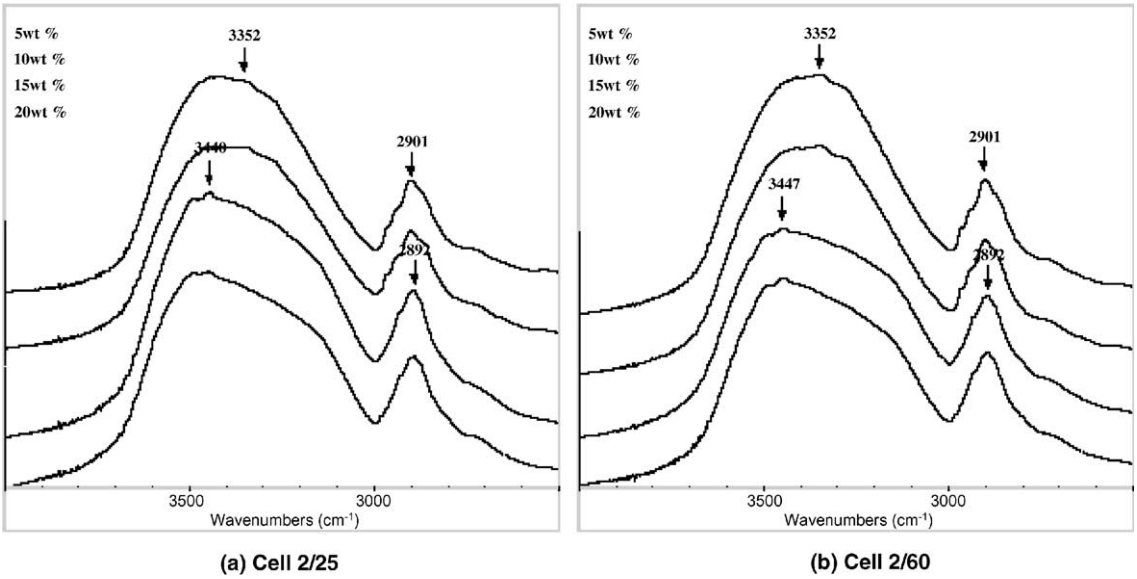

Figure 6. FTIR spectra (4000–2500 cm^{-1}) of Cell 2 samples prepared at different NaOH concentrations and temperatures of (a) 25 °C and (b) 60 °C.

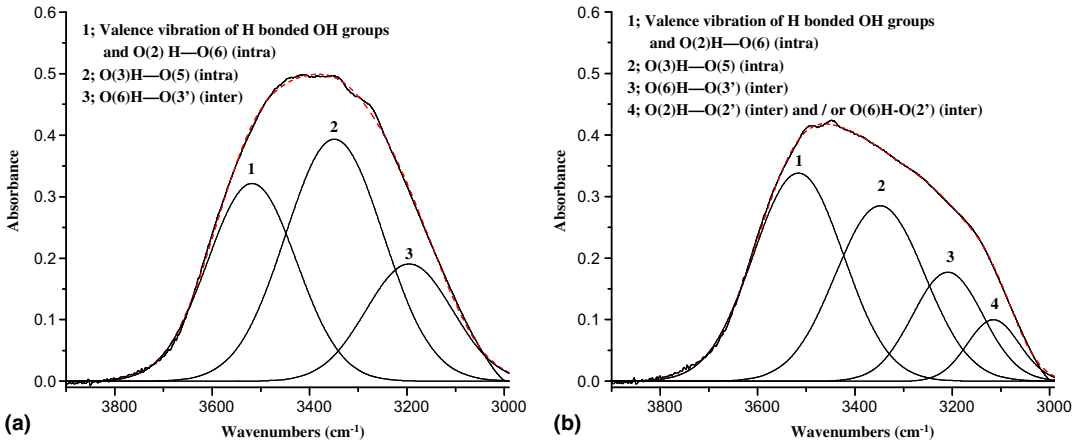

Figure 7. Resolution of hydrogen-bonded OH stretching for (a) cellulose I [Cell 2/60 with 5 wt % NaOH] and (b) cellulose II [Cell 2/60 with 15 wt % NaOH].

wood (and cellulose)[27] and viscose fiber,[28] respectively. An absorbance increase of the band at 897 (or 894) cm^{-1} was also observed by transformation.[25] Similarly, the band at 1165 cm^{-1} assigned as C–O–C stretching at the β-(1→4)-glucosidic linkage is shifted to 1162 cm^{-1}.[25,29,48] The band at 1337 cm^{-1} is not shifted, and the absorbance of this band is slightly decreased by the transformation (Table 2). From the resolution of hydrogen-bonded OH stretching as shown in Figure 7, the environment of C-3 is indistinguishable from that of C-2 and rarely changed by transformation. Combining the above findings, the band at 1337 cm^{-1} is assigned as the C–O–H bending at C-2 or C-3. The FTIR absorbance and wave number at maximum absorbance of C–O–H bending in plane at C-6 is changed by transformation of the band at 1431 (1419) cm^{-1}, which arises by changing the environment at C-6.

3.3. The change of CI and crystallite size by transformation

Treatment of cellulose with NaOH and CO_2 changes the CI as well as the crystal system of the cellulose. The CIs of Cell 1 and Cell 1-C obtained from X-ray diffraction curves, as shown in Figure 1a are 0.65 and 0.73, respectively. Figure 9a shows CI curves of Cell 2 and Cell 2-C calculated from X-ray diffraction curves of Figure 2. The CI of Cell 2 and Cell 2-C decreased up to 15 and 10 wt % of NaOH, respectively. In addition, the CIs of Cell 2/25-C and Cell 2/60-C are smaller than those of

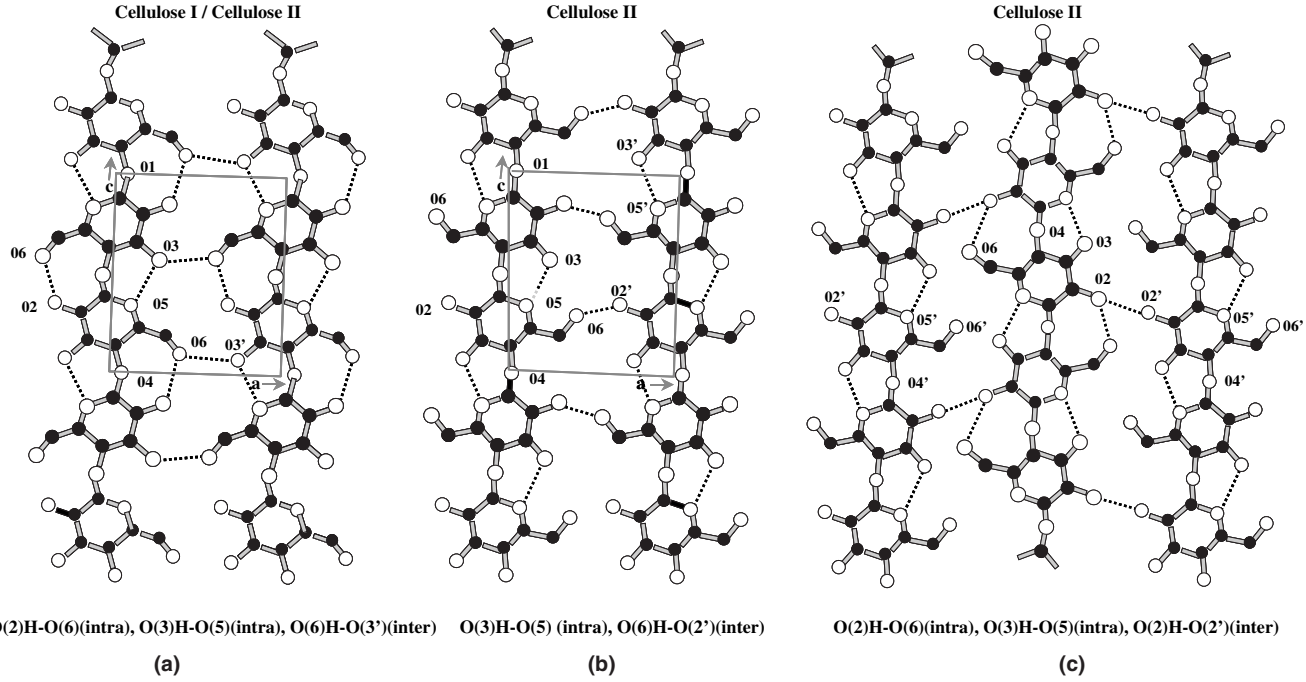

Figure 8. Proposed hydrogen-bonding patterns by Kolpak and Blackwell:[7] (a) 020 plane ('down' chains), (b) 020 plane ('up' chains), and (c) 110 plane.

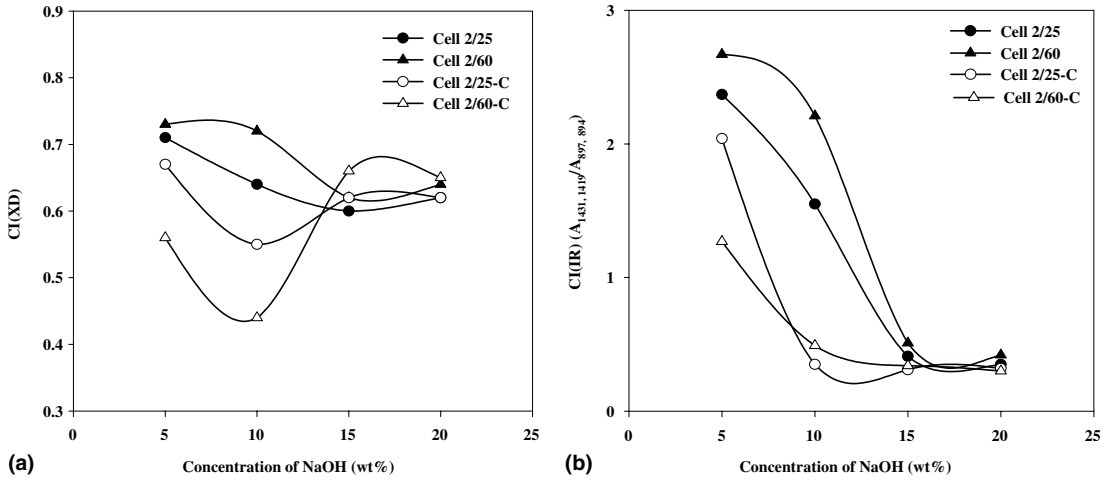

Figure 9. (a) CI(XD) and (b) CI(IR) ($A_{1431,1419}/A_{897,894}$) of Cell 2 and Cell 2-C prepared at different NaOH concentrations and temperatures.

Cell 2/25 and Cell 2/60 at <15 wt % NaOH treatment, but converge at ⩾15 wt %. As shown in Figures 2 and 9, a small portion of cellulose crystalline structure is changed to an amorphous region by NaOH and CO_2 treatment.

The absorbances at 1430 cm^{-1} and 894 cm^{-1} are sensitive to the amount of crystalline versus amorphous structure in the cellulose, that is, broadening of these bands reflects more disordered structure.[50] The absorbance ratio A_{1430}/A_{900} was defined as an empirical CI.[28,32] Compared with the diffraction patterns as shown in Figure 2, the ratio $A_{1431,1419}/A_{897,894}$ (Fig. 9b) is related to the proportion of cellulose I. The shape of CI(IR) in Figure 10b is quite different from CI(IR) in Figure 10a. CI(IR) of the Cell 2 decreases with the treatment of NaOH up to 15 wt % and then remains constant at ⩾15 wt % NaOH as shown in Figure 10a. In Figure 10b, CI(IR) of the Cell 2-C is larger than Cell 2 treated up to 10 wt % NaOH. Most of the bands in Table 2 show the absorbance change when the cellulose I lattice is transformed to the cellulose II lattice. The absorbance ratio of the bands at 1375 and 2900 cm^{-1} is also reported to be significant for CI.[37] As with $A_{1431,1419}/A_{897,894}$ and $A_{1263}/A_{1202,1200}$, all of bands listed in Table 2 are

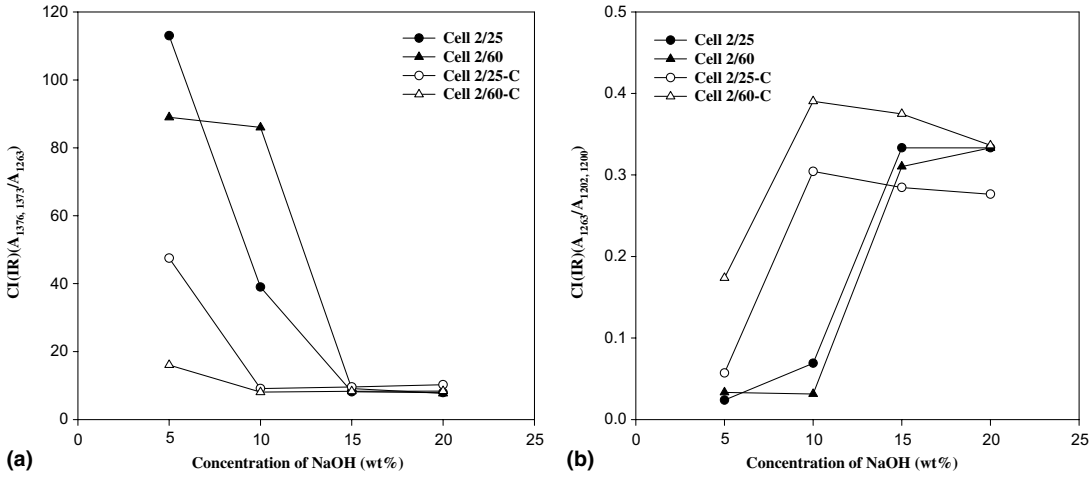

Figure 10. (a) CI(IR) ($A_{1376,1373}/A_{1263}$) and (b) CI(IR) ($A_{1263}/A_{1202,1200}$) of Cell 2 and Cell 2-C prepared at different NaOH concentrations and temperatures.

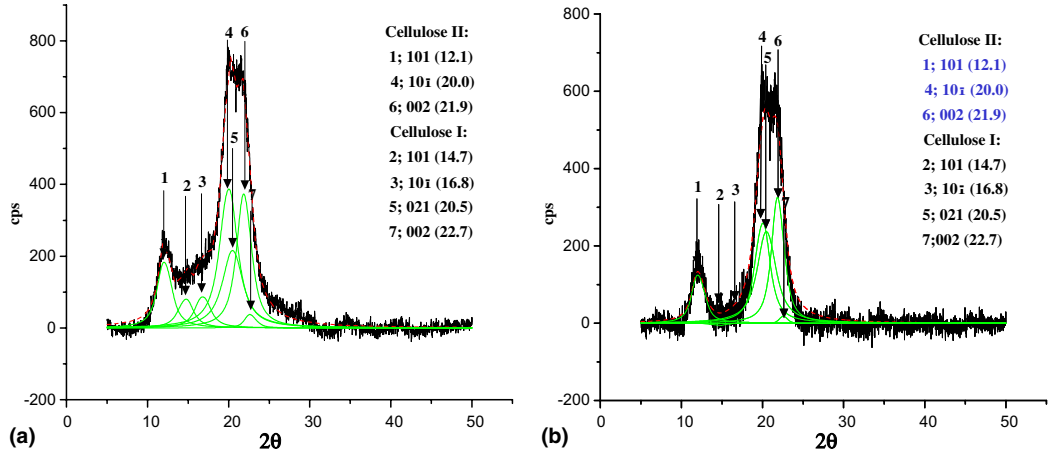

Figure 11. Resolution of X-ray diffraction curves of Cell 2/25-C prepared at 10 wt % NaOH treatment (a) as analyzed and (b) corrected for amorphous reflection.

calculated by absorbance ratio evaluated as CI. Typically, the absorbance ratios show a decrease or an increase with an increase of NaOH concentration as shown in Figure 10. As in Figure 9b, the CI(IR) in Figure 10a decreases with an increase of NaOH concentration, indicating a decrease in the cellulose I portion. In contrast, the CI(IR) in Figure 10b shows an increase of absorbance ratio, which relates the transformation to a cellulose II lattice.

X-ray diffraction curve as analyzed is the sum of all crystal allomorphs in the cellulose sample. In this study, the resolution of cellulose is approached with and without baseline correction related to amorphous reflection. The peak of X-ray diffraction curves are resolved as shown in Figure 11. Figure 12 shows the CI(XD) components derived from the method as shown in Figure 11a. By the baseline correction due to amorphous reflection (Fig. 11b), CI(XD) components are almost the same as Figure 12. This result also shows incomplete transformation (cellulose I→cellulose II) for the NaOH-treated and/or CO_2-treated celluloses used in this study. The correlation between CI(XD) components obtained from both methods are shown in Figure 13. The linearity for both CI(XD) components supports the contention that peak resolution without baseline correction of Figure 11a is more convenient for the correlation between CI(XD) and CI(IR) compared with Figure 11b, because the additional step such of baseline correction can be avoided.

Many researchers have correlated CI(XD) and CI(IR) measured by some absorbance or absorbance ratios of FTIR such as 2900, 1263, 1370, 896, and 670 cm^{-1}.[27,28,32,51–56] In addition to the absorbance ratios such as $A_{1431,1419}/A_{897,894}$ and $A_{1263}/A_{1202,1200}$, we evaluated all the correlations between CI(XD-CI) (or CI(XD-CII)) and CI(IR) obtained without baseline correction and absorbance ratios using all the characteristic

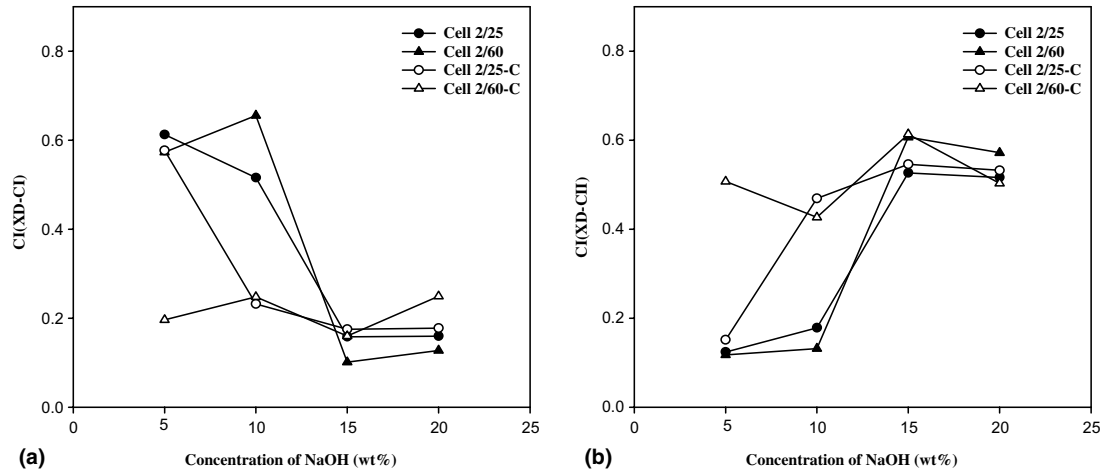

Figure 12. CI(XD) resolved from X-ray diffraction curves of Cell 2 and Cell 2-C prepared at different NaOH concentrations and temperatures.

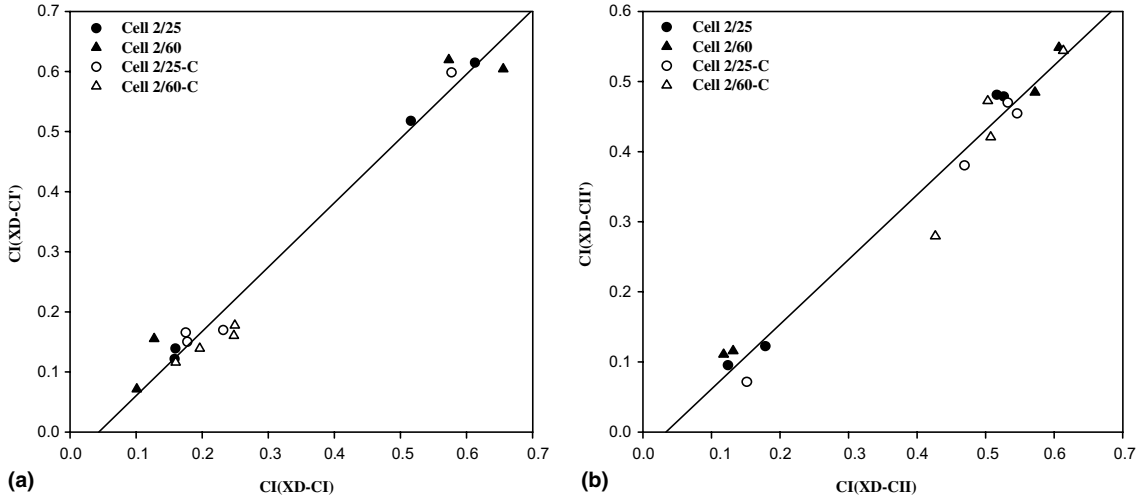

Figure 13. Correlation between (a) CI(XD-CI) or CI(XD-CII) (without baseline correction) and (b) CI(XD-CI′) or CI(XD-CII′) (with baseline correction), respectively [correlation coefficient 0.97 for both (a) and (b)].

bands of Table 2, respectively. Figure 14 shows typical correlation curves between CI(IR) and CI(XD-CI)/CI(XD-CII) from the data represented in Figures 9a and 10b. The coefficient of 0.86 is shown for the correlation curve between CI(IR) ($A_{1431,1419}/A_{897,894}$) and CI(XD-CI) in Figure 14a. As the same approach, the coefficient of similar value but negative slope is maintained for the correlation between CI(IR) ($A_{1431,1419}/A_{897,894}$) and CI(XD-CII). The correlation curve between CI(IR) ($A_{1263}/A_{1202,1200}$) and CI(XD-CI) shows a negative slope and a coefficient of 0.84 (Fig. 14b). Other correlation coefficients larger than 0.8 (all positive slopes) are listed in Table 3. Some internal standards such as 2900, 1263, 894 cm^{-1} have already been reported.[27,28,32] Comprehensive evaluation for the bands listed in Table 2 derives that the bands at 2901 (2802), 1373 (1376), 897 (894), 1263, 668 cm^{-1} are good for the internal standards of CI(IR), which increase the correlation coefficient. Many of the bands show similar information related to the transformation. As a typical example shown in Figure 15, the correlation between the absorbance ratios of the same internal standard (or denominator) approaches unity.

Using a pair of bands showing peak shifts, each fraction of two absorbances can be assigned as an alternate of CI(IR). The fractions of both absorbances are well correlated with CI(XD) as shown in Figures 16 and 17. The correlation coefficient between CI(IR) and CI(XD-CII) in Figure 16b is higher than that in Figure 14a. Similarly, the coefficient of CI(IR) and CI(XD-CI) in Figure 17a is higher than that in Figure 14b. This tendency is also confirmed in the other pair of bands listed

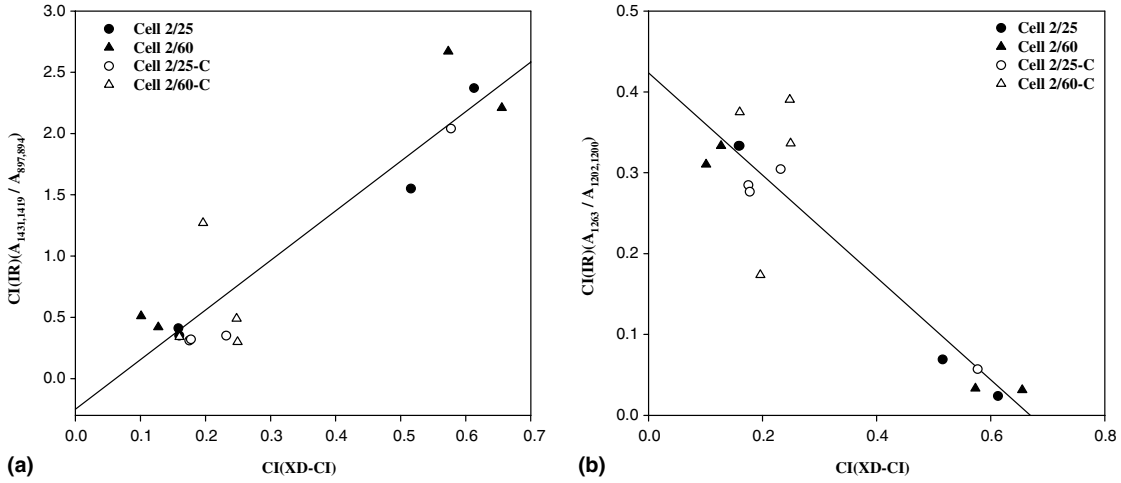

Figure 14. Correlation between (a) CI(XD-CI) and CI(IR) ($A_{1431,1419}/A_{897,894}$) or (b) CI(IR) ($A_{1263}/A_{1202,1200}$) of Cell 2 and Cell 2-C [correlation coefficient (a) 0.86 and (b) 0.84].

Table 3. The absorbance ratios suggested for the evaluation of CI[a]

Internal standard (cm^{-1})	Related bands (cm^{-1})[correlation coefficient]	
	CI(XD-CI)	CI(XD-CII)
2901 (2892)	1431 (1419)[0.83], 1058[0.83], 713[0.81]	1263[0.81]
1373 (1376)	1058[0.83]	—
1202 (1200)	—	1263[0.83]
897 (894)	1431 (1419)[0.86], 1373 (1376)[0.82], 1282 (1278)[0.80], 1058[0.81], 713[0.89]	—
1263	1431 (1419)[0.81], 1373 (1376)[0.82], 1032 (1019)[0.81], 1058[0.81], 713[0.85]	—
668	713[0.85]	—

[a] Correlation coefficient with CI(XD-CI) or CI(XD-CII) $\geqslant$ 0.80.

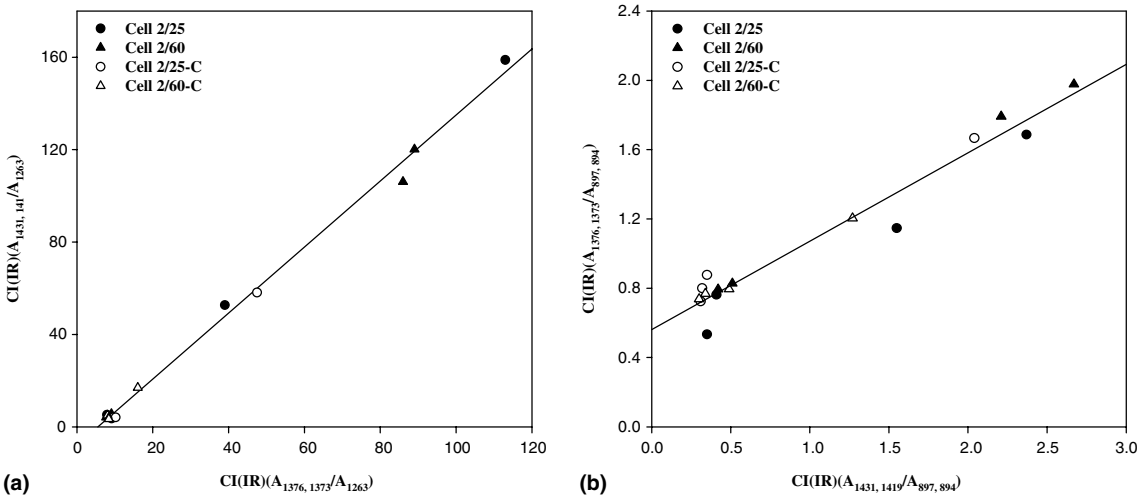

Figure 15. Correlation between (a) CI(IR) ($A_{1431,1419}/A_{1263}$) and CI(IR) ($A_{1376,1373}/A_{1263}$)/CI(IR) ($A_{1431,1419}/A_{897,\ 894}$) and (b) CI(IR) ($A_{1376,1373}/A_{897,894}$) of Cell 2 and Cell 2-C [correlation coefficient (a) 0.99 and (b) 0.96].

in Table 3. Correlated with CI(XD) values in the range of 0–1, the newly defined CI(IR) gives a higher coefficient than the CI(IR) defined as an absorbance ratio.

Figure 18 shows the crystallite size of Cell 2 and Cell 2-C obtained at several reflections. The crystallite size is decreased to a constant value when cellulose is treated

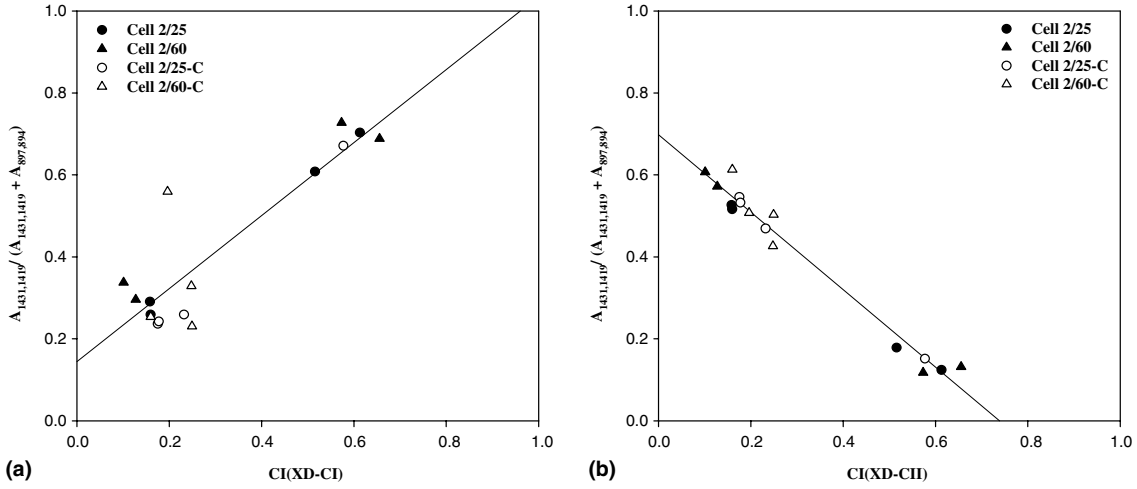

Figure 16. Correlation between (a) CI(XD-CI) or (b) CI(XD-CII) and $A_{1431,1419}/(A_{1431,1419}+A_{897,894})$ of Cell 2 and Cell 2-C [correlation coefficient (a) 0.81 and (b) 0.97].

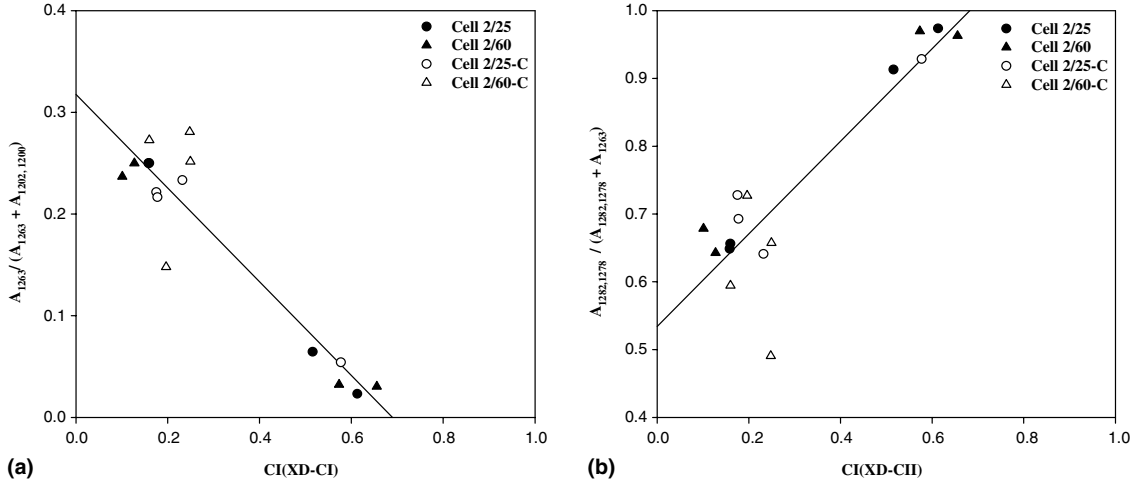

Figure 17. Correlation between CI(XD-CI) and (a) $A_{1263}/(A_{1263}+A_{1202,1200})$ or (b) $A_{1282,1278}/(A_{1282,1278}+A_{1263})$ of Cell 2 and Cell 2-C [correlation coefficient (a) 0.87 and (b) 0.79].

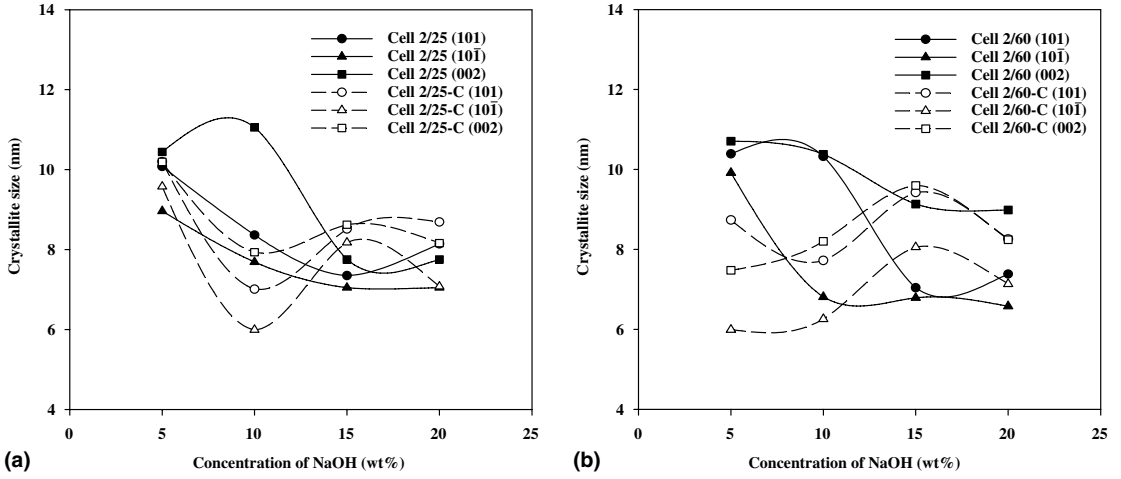

Figure 18. Crystallite size of (a) Cell 2/25 and Cell 2/25-C and (b) Cell 2/60 and Cell 2/60-C.

with $\geqslant$15 wt % NaOH. The crystallite size of Cell 2-C (cellulose II) is smaller than that of Cell 2 (cellulose I) treated with 5–10 wt % NaOH. In contrast, the crystallite size of Cell 2-C (cellulose II) is larger than that of Cell 2 (cellulose II) treated at 15–20 wt % NaOH. X-ray diffraction pattern gives information related to the size and perfection of the crystalline domains. It is known that the crystallite size of cellulose II is smaller than that of cellulose I.[1]

4. Conclusions

The crystalline structure of the cellulose treated with NaOH and CO_2 was analyzed by wide-angle X-ray diffraction analysis and FTIR spectroscopy. The transformation to cellulose II was observed by X-ray diffraction for cellulose treated with 15–20 wt % NaOH or 5–20 (or 10–20) wt % NaOH with CO_2.

From the FTIR spectra, the bands at 3352, 2901, 1431, 1373, 1282, 1236, 1202, 1165, 1032, and 897 cm^{-1} are shifted to 3447, 2892, 1419, 1376, 1278, 1228, 1200, 1162, 1019, and 894 cm^{-1}, respectively. These bands may be influenced by the change of inter- or intramolecular hydrogen bonds during the transformation. Many of the FTIR bands including 2901, 1431, 1282, 1236, 1202, 1165, 1032, and 897 cm^{-1} were shifted to higher wave number (by 2–13 cm^{-1}), while the bands at 3352, 1373, and 983 cm^{-1} were shifted to lower wave number (by 3–95 cm^{-1}). At the same time, the absorbances of the bands at 1337, 1114, and 1058 cm^{-1} are decreased and those at 1263, 993, and 668 are increased. The FTIR spectra of hydrogen-bonded OH stretching vibrations at around 3352 cm^{-1} are resolved into three bands for cellulose I and four bands for cellulose II, assuming that all the vibration modes follow Gaussian distribution. The bands of 1 (3518 cm^{-1}), 2 (3349 cm^{-1}), and 3 (3195 cm^{-1}) are related to the sum of the valence vibrations of an H-bonded OH group and the intramolecular hydrogen bond 2-OH$\cdots$O-6, intramolecular hydrogen bond of 3-OH$\cdots$O-5 and the intermolecular hydrogen bond of 6-OH$\cdots$O-3′, respectively. Compared with the bands of cellulose I, a new band of 4 (3115 cm^{-1}) related to intermolecular hydrogen bond of 2-OH$\cdots$O-2′ and/or intermolecular hydrogen bond of 6-OH$\cdots$O(2′) in cellulose II appeared.

CI(XD) of the cellulose treated is slightly decreased with an increase in NaOH concentration. With the CO_2 treatment that follows, it is considerably decreased up to 10 wt % NaOH. Resolution of CI(XD) was performed to obtain the portion of the cellulose I and cellulose II lattice. From the correlation between CI(IR) and CI(XD-CI) (or CI(XD-CII)), the bands at 2901 (2802), 1373 (1376), 897 (894), 1263, 668 cm^{-1} are good for internal standards of CI(IR). Using a pair of bands showing peak shifts, each fraction of two absorbances can be assigned as an alternate of CI(IR). Correlated with CI(XD) values in the range of 0–1, the newly defined CI(IR) gives a higher coefficient than the CI(IR) defined as an absorbance ratio. Partial transformation to cellulose II by NaOH or NaOH/CO_2 treatment onto cellulose is shown by the resolved FTIR spectra of hydrogen-bonded OH stretching vibrations and the resolved X-ray diffraction patterns.

The crystallite size is decreased to a constant value for Cell 2 treated at higher than 15 wt % NaOH. The crystallite size of Cell 2-C (cellulose II) is smaller than that of Cell 2 (cellulose I) treated at 5–10 wt % NaOH. On the contrary, the crystallite size of Cell 2-C (cellulose II) is larger than that of Cell 2 (cellulose II) treated at 15–20 wt % NaOH.

Acknowledgement

This work was supported by grant No. R01-2001-00522-0 from the Korea Science & Engineering Foundation.

References

1. Klemm, D.; Philipp, B.; Heinze, T.; Heinze, U.; Wagenknecht, W. In *Comprehensive Cellulose Chemistry*; Wiley–VCH: Weinheim, 1998; Vol. 1, pp 9–25.
2. Zugenmaier, P. *Prog. Polym. Sci.* **2001**, *26*, 1341–1417.
3. Jähn, A.; Schröder, M. W.; Füting, M.; Schenzel, K.; Diepenbrock, W. *Spectrochim. Acta, Part A* **2002**, *58*, 2271–2279.
4. Dinand, E.; Vignon, M.; Chanzy, H.; Heux, L. *Cellulose* **2002**, *9*, 7–18.
5. Moncrieff, R. W. In *Man-Made Fibres*, 6th ed.; Newnes–Butterworths: London, 1975; pp 162–299.
6. Kroschwitz, J. I. In *Polymers: Fibers and Textiles, A Compendium*; John Wiley & Sons: New York, 1990, pp 746–772.
7. Kolpak, F. J.; Blackwell, J. *Macromolecules* **1976**, *9*, 273–278.
8. Nishiyama, Y.; Langan, P.; Chanzy, H. *J. Am. Chem. Soc.* **2002**, *124*, 9074–9082.
9. Nishiyama, Y.; Sugiyama, J.; Chanzy, H.; Langan, P. *J. Am. Chem. Soc.* **2003**, *125*, 14300–14306.
10. Gümüskaya, E.; Usta, M.; Kirci, H. *Polym. Degrad. Stab.* **2003**, *81*, 559–564.
11. Stipanovic, A. J.; Sarko, A. *Macromolecules* **1976**, *9*, 851–857.
12. Fengel, D. *Papier* **1993**, *47*, A695–A702.
13. Fengel, D.; Jakob, H.; Strobel, C. *Holzforschung* **1995**, *49*, 505–511.
14. Fink, H. D.; Fanter, D.; Philipp, B. *Acta Polym.* **1985**, *36*, 1–8.
15. Gert, E. V.; Socarras-Morales, A.; Zubets, O. V.; Shishonok, M. V.; Torgashov, V. I.; Matyulko, A. V.; Kaputski, F. N. *Cellul. Chem. Technol.* **2001**, *35*, 417–427.
16. Matsuo, M.; Sawatari, C.; Iwai, Y.; Ozaki, F. *Macromolecules* **1990**, *23*, 3266–3275.

17. Richter, U.; Krause, T.; Schempp, W. *Papier* **1992**, *46*, A318–A323.
18. Wakida, T.; Lee, M.; Park, S. J.; Hayashi, A. *Sen-I Gakkaishi* **2002**, *58*, 304–307.
19. Sarko, A.; Muggli, R. *Macromolecules* **1973**, *7*, 486–494.
20. Sugiyama, J.; Vuong, R.; Chanzy, H. *Macromolecules* **1991**, *24*, 4168–4175.
21. Atalla, R. H.; VanderHart, D. L. *Solid-State Nucl. Magn. Reson.* **1999**, *15*, 1–19.
22. Cael, J. J.; Gardner, K. H.; Koenig, J. L.; Blackwell, J. *J. Chem. Phys.* **1975**, *62*, 1145–1153.
23. Proniewicz, L. M.; Paluszkiewicz, C.; Weselucha-Birczyńska, A.; Majcherczyk, H.; Barański, A.; Konieczna, A. *J. Mol. Struct.* **2001**, *596*, 163–169.
24. Kondo, T.; Sawatari, C. *Polymer* **1996**, *37*, 393–399.
25. Nelson, M. L.; O'Connor, T. *J. Appl. Polym. Sci.* **1964**, *8*, 1311–1324.
26. Ruan, D.; Zhang, L.; Mao, Y.; Zeng, M.; Li, X. *J. Membr. Sci.* **2004**, *241*, 265–274.
27. Schwanninger, M.; Rodrigues, J. C.; Pereira, H.; Hinterstoisser, B. *Vib. Spectrosc.* **2004**, *36*, 23–40.
28. Colom, X.; Carrillo, F. *Eur. Polym. J.* **2002**, *38*, 2225–2230.
29. Kačuráková, M.; Capek, P.; Sasinková, V.; Wellner, N.; Ebringerová, A. *Carbohydr. Polym.* **2000**, *43*, 195–203.
30. Wellner, N.; Kačuráková, M.; Malovíková, A.; Wilson, R. H.; Belton, P. S. *Carbohydr. Res.* **1998**, *308*, 123–131.
31. Kačuráková, M.; Smith, A. C.; Gidley, M. J.; Wilson, R. H. *Carbohydr. Res.* **2002**, *337*, 1145–1153.
32. Åkerholm, M.; Hinterstoisser, B.; Salmén, L. *Carbohydr. Res.* **2004**, *339*, 569–578.
33. Fengel, D.; Strobel, C. *Acta Polym.* **1994**, *45*, 319–324.
34. Newman, R. H.; Davidson, T. C. *Cellulose* **2004**, *11*, 23–32.
35. Krässig, H. A. In *Cellulose: Structure, Accessibility and Reactivity, Polymer Monographs V11*; Gordon and Breach Science Publishers: Yverdon, Switzerland, 1993; pp 88–90, 100–107, and 123–125.
36. Oh, S. Y.; Yoo, D. I.; Shin, Y.; Lee, W. S.; Jo, S. M. *Fibers Polym.* **2002**, *3*, 1–7.
37. Oh, S. Y.; Yoo, D. I.; Seo, G. *Carbohydr. Res.* **2005**, *340*, 417–428.
38. Nishiyama, Y.; Kuga, S.; Okano, T. *J. Wood Sci.* **2000**, *46*, 452–457.
39. Chen, H.; Yokochi, A. *J. Appl. Polym. Sci.* **2000**, *76*, 1466–1471.
40. Kondo, T. In *Hydrogen Bonds in Cellulose and Cellulose Derivatives. Polysaccharides. Structural Diversity and Functional Versatility*; Marcel Dekker: New York, 1998; pp 131–172.
41. Fengel, D. *Holzforschung* **1993**, *47*, 103–108.
42. Fengel, D. In *Cellulosics: Chemical, Biochemical and Material Aspects*; Kennedy, J. F., Phillips, G. O., Williams, P. A., Eds.; Ellis Horwood: New York, 1993; pp 135–140.
43. Fengel, D. *Holzforschung* **1992**, *46*, 283–288.
44. Isogai, A.; Usuda, M.; Kato, T.; Uryu, T.; Atalla, R. H. *Macromolecules* **1989**, *19*, 513.
45. Langan, P.; Nishiyama, Y.; Chanzy, H. *J. Am. Chem. Soc.* **1999**, *121*, 9940–9946.
46. Raymond, S.; Kvick, Å.; Chanzy, H. *Macromolecules* **1995**, *28*, 8422–8425.
47. Freytag, R.; Donzé, J. J. In *Chemical Processing of Fibers and Fabrics. Fundamentals and Preparation. Part A*; Lewin, M., Sello, S. B., Eds.; Handbook of Fiber Science and Technology; Marcel Dekker: New York, 1983; Vol. I, pp 134–148.
48. CaO, Y.; Tan, H. *J. Mol. Struct.* **2004**, *705*, 189–193.
49. Liang, C. Y.; Marchessault, R. H. *J. Polym. Sci.* **1959**, *39*, 269–278.
50. O'Connor, R. T.; DuPre, E. F.; Mithcum, D. *Text. Res. J.* **1958**, *28*, 383.
51. Schultz, T. P.; McGinnis, G. D.; Bertran, M. S. *J. Wood Chem. Technol.* **1985**, *5*, 543–557.
52. Evans, R.; Newman, R. H.; Roick, Ute C.; Suckling, I. D.; Wallis, A. F. A. *Holzforschung* **1995**, *49*, 498–504.
53. Gu, L.; Ruan, R.; Chen, P.; Wilcke, W.; Addis, P. *Trans. ASAE* **2001**, *44*, 1707–1712.
54. Richter, U.; Krause, T.; Schempp, W. *Angew. Makromol. Chem.* **1991**, *185*, 155–167.
55. Takács, E.; Wojnárovits, L.; Földváry, C.; Borsa, J.; Sajó, I. *Res. Chem. Intermed.* **2001**, *27*, 837–845.
56. Tasker, S.; Badyal, J. P. S.; Backson, S. C. E.; Richards, R. W. *Polymer* **1994**, *35*, 4717–4721.